# Lab on a Chip

Accepted Manuscript






ROYAL SOCIETY OF CHEMISTRY

www.rsc.org/loc

Lab on a Chip

ARTICLE

# Droplet-in-oil array for picoliter-scale analysis based on sequential-inkjet printing

Received 00th January 20xx,
Accepted 00th January 20xx

DOI: 10.1039/x0xx00000x

www.rsc.org/

Yingnan Sun[a], Xiaodong Chen[b], Xiaoguang Zhou[a], Jinbiao Zhu[c] and Yude Yu*[,a]

In recent years, inkjet printing, as a new method to fabricate microdroplet microarrays, is being increasingly applied in the fields of biochemical diagnostics. To further improve the general applicability of inkjet printing technology in fabricating biochemical chips, in this work, we introduce a model to describe the multiple injection procedure implemented with the inkjet printing approach, with experimental verification. The multiple injection model demonstrates a new sequential-inkjet printing method that generates picoliter-scale multicomponent droplet-in-oil arrays with multistep printing on uniform planar substrates. Based on our previous work on double-inkjet printing, this technique adapts piezoelectric inkjet printing technology to fabricate an oil droplet array, into which multiple precise injections of secondary droplets with different compositions and volumes can be automatically printed in the required sequence, simultaneously addressing the evaporation issues associated with printing picoliter droplets without external assistance. In this paper, we first describe the theory and characterize the model, which account for the basic principles of sequential-inkjet printing, as well as validate the design in terms of multiple injections, droplet fusion, and rapid mixing. The feasibility and effectiveness of the method are also demonstrated in a dual-fluorescence assay and a β-galactosidase enzyme inhibition assay. We believe that applying the sequential-inkjet printing methodology in existing inkjet printing devices will enhance their use as universal diagnostic tools as well as accelerate the adoption of inkjet printing in multistep screening experiments.



[a] *State Key Laboratory on Integrated Optoelectronics, Institute of Semiconductors, Chinese Academy of Sciences. P.O. Box 912, Beijing 100083, P.R. China*
[b] *State Key Laboratory of Nonlinear Mechanics, Institute of Mechanics, Chinese Academy of Sciences, No. 15 Beisihuanxi Road, Beijing 100190, P.R. China*
[c] *Institute of Electronics, Chinese Academy of Sciences, No. 19 North 4th Ring Road West, Beijing 100190, P.R. China*
* Corresponding Author: E-mail: yudeyu@semi.ac.cn. Fax: +86-10-82305052; Tel: +86-10-82304979.

† Electronic Supplementary Information (ESI) available: Figure S1, Movie S1. See DOI: 10.1039/b000000x/

## Introduction

This paper describes a new sequential-inkjet printing model for generating picoliter multicomponent droplet-in-oil arrays on uniform planar substrates. Printing technology, especially inkjet printing, is an alternative to microfluidic technology, and has the advantages of both high throughput and precise control of small volumes, which satisfy the critical demands for chemical and biomedical diagnostic assays, especially in fields such as drug discovery. The technique does not require the use of masks and also affords high positional accuracy.[1] It has been employed in many areas as one of the most promising methods for efficient microarray fabrication through the generation and precise control of droplet volumes. Pignataro *et al*. successfully employed inkjet printing to construct drug–target recognition assays in a simple microarray format.[2,3] Uchiyama *et al*. combined inkjet technology with a multicapillary plate to develop a chemiluminescence immunoassay.[4]

Despite these achievements, however, inkjet-based array formation is still not being widely applied in chemical and biological research. This is because the application of this technology still confronts intractable challenges. One issue is the evaporation of droplets during array fabrication. Evaporation effects typically prevent the extreme scale reduction of droplet reactions to picoliter volumes. Specific strategies have been devised to address this problem, including the introduction of an ultrasonic humidifier,[5,6] or the use of additive chemicals such as glycerol[3,7] or dimethyl sulfoxide (DMSO)[8] to maintain constant water content. However, these approaches run the risk of cross-contamination or suffer from limitations due to incompatibility with enzyme species, which limits the applicability of inkjet printing for most screening assays.[9] In our previous work, we developed a novel double-inkjet printing method to thoroughly prevent picoliter droplet evaporation during array fabrication by generating droplet-in-oil arrays.[10] This approach enhanced and extended the universal applications of inkjet printing.

The described method, however, just involved a one-time successful liquid injection to form the droplet-in-oil structure, which would not be suitable for a multistep biochemical assay. Many experiments require the evaluation of multiple samples or reagents, or use different mixing-ratio conditions.[11] The most commonly used microwell structures and microfluidic devices are integrated in closed microchannels in order to stably store small amounts of liquid;[12–15] this limits the ability to repeatedly add reagents or select specific droplets from the closed channels. Since printing technology has the advantage of open operation, allowing easy access to the contents, it is necessary and meaningful to realize multistep droplet manipulation based on the inkjet printing approach. To accomplish this, Fang *et al*. developed a sequential operation droplet array (SODA) system based on capillary-syringe modules.[16,17] In this method, liquid droplets containing bioactive molecules were dispensed by immersing a capillary tip in an oil layer to create an oil-covered droplet array installed on an *x*–*y*–*z* translation stage. However, such an approach is hampered scale reduction by liquid contact during dispensing, with consequent contamination issues. Pignataro *et al*. employed inkjet printing for the fabrication of sub-nanoliter droplet-to-droplet arrays.[2,3] In this method, due to the high hygroscopicity of glycerol, liquid spots are stable during both the multilayer-assembly and the execution of the assay. However, none of these printing methods can provide precise and reliable multistep droplet dispensing while exhibiting all of the following features: non-contact liquid dispensing capability, absence of evaporation issues without the assistance of additives, and capability of multistep/sequential droplet assembly.

Here, we introduce a sequential-inkjet printing model to describe the multistep picoliter droplet-in-oil assembly generated with inkjet printing technology on planar substrates. This sequential-inkjet printing model utilizes piezoelectric inkjet printing equipment to first fabricate an oil droplet array, which is then subjected to multiple precise injections of aqueous droplets with different compositions and volumes in the required sequence. If the system satisfies certain conditions, the successively injected droplets will penetrate an oil drop and merge into one larger aqueous droplet therein. In summary, the sequential-inkjet printing approach has the following beneficial features that have not been combined previously in a single method:

(a) This model employs inkjet printing technology to realize multistep/sequential droplet printing with



 

high control over the size and composition of each droplet.

(b) The sequential-inkjet process completely addresses the evaporation issues of picoliter-scale droplets without additional assistance, which makes this platform suitable for a wider range of chemical and biological assay systems.

(c) This approach serves as a contact-free sample printing method capable of performing multiple liquid injections, which is totally different from previous dispensing systems.[16,17] By employing a droplet ejected at high speed from a nozzle, the sequential-inkjet approach deposits droplets on the top of the chip without the need to contact the oil or reagents, thus avoiding cross-contamination. Furthermore, because of the non-contact printing mode, only an *x*–*y* stage is needed for the process, which significantly improves the preparation efficiency compared to previous work.[16,17]

Our primary objective in this work was to employ inkjet printing technology to develop a non-contact and sequential picoliter droplet printing model in order to further improve the universality of inkjet printing applications in biochemical analysis. In this study, we first develop a three-phase model of sequential-inkjet printing for multicomponent droplet formation. Then, the injection rate and sample parameters are investigated using a flow dynamics simulation to identify the optimized conditions and better understand the process. Finally, we evaluate the efficiency and reliability of this sequential-inkjet printing model in a simple microarray format by performing successful enzyme inhibition assays.

## Experimental Section

### Chemicals and Materials

All solvents and chemicals were reagent grade unless otherwise stated. Deionized water was used throughout. Mineral oil (Sigma Aldrich, M8410), sodium phosphate monobasic ($NaH_2PO_4$), sodium phosphate dibasic ($Na_2HPO_4$), HCl, tris(hydroxymethyl)aminomethane (Tris), 1*H*,1*H*,2*H*,2*H*-perfluorooctyltriethoxysilane, DMSO, diethylenetriaminepentaacetic acid (DTPA), and β-galactosidase from *Escherichia coli* (β-gal, 250 units/mg) were obtained from Sigma-Aldrich (Shanghai, China). Fluorescein digalactoside (FDG) and Alexa Fluor® 488 dye were obtained from Molecular Probes (Eugene, OR). ROX dye was purchased from Toyobo (Shanghai, China). Silicon wafers were purchased from Yuxin Co. Ltd. (Tianjin, China). Piezoelectric inkjet nozzles with diameters of 50 μm (MJ-AT-01-50) and 30 μm (MJ-AT-01-30) were obtained from MicroFab Technologies, Inc. (Plano, TX).

### Substrate Preparation

Distinguished from previous studies, we developed a planar substrate with a uniformly hydrophobic and oleophobic surface in place of a hydrophilic-in-hydrophobic pattern or microwell array to fabricate picoliter droplet-in-oil arrays. First, to prevent the adsorption of enzyme reagents onto the silicon surface,[18] a 300 nm layer of $SiO_2$ was grown on the silicon wafer by thermal oxidation at 1100°C for 1 h. Then, a rectangular area (2 cm × 1.5 cm) of the $SiO_2$ layer was gas-phase silanized in a desiccator with 1*H*,1*H*,2*H*,2*H*-perfluorooctyltriethoxysilane for 2 min at 85°C, to impart hydrophobic and oleophobic properties to the surface. By these surface treatments, optimum contact angles of 120° and 73° for water and mineral oil,[10] respectively, were achieved.

### Experimental Apparatus

We built an inkjet-based printing system, which is an improvement upon the basic Jetlab® 4 inkjet platform (MicroFab).[19] This printing system consists of three major components (Fig. S1, ESI†): (1) an inkjet-dispensing device coupled with pressure and electric control blocks. Software was used to control the device by adjusting different parameters; (2) a stroboscopic–optics subsystem, designed to observe the formation and trajectories of droplets in flight with the assistance of a pulsed LED for illumination. Horizontal and vertical optics subsystems were designed to ensure the accurate alignment of the nozzle orifice with preprinted oil droplets; and (3) a two-dimensional precision displacement platform (M406.4PD, Physik Instrumente, Germany) with a minimum incremental motion of 0.25 μm (Fig. S2, ESI†). The silicon substrate was placed on the *x*–*y* translation stage. The complete droplet-array generation was performed on this modified inkjet platform equipped with task-specific nozzles. The nozzle orifice diameters were 30 and 50 μm for reagent and oil droplet formation, respectively.

All bright and fluorescence images of the droplet arrays were obtained with an Olympus microscope (TE2000, Olympus, Japan) equipped with a CCD

camera (DP72, Olympus) and a filter set (460/20 nm for fluorescence excitation and 532/30 nm for emission collection of Alexa Fluor® 488 dye; and 550/20 nm for excitation and 612 nm/long-pass for emission collection of the ROX dye).

**Model for Sequential-inkjet Printing**

To perform a numerical simulation of the droplet-in-oil formation based on sequential-inkjet printing, a three-phase model was developed based on the general numerical framework of the Gerris Flow Solver.[20] The model can describe flow problems with three fluids and three kinds of interfaces. In addition, a thickness-based refinement method[21] was combined with a gradient-based refinement of the interfaces to improve the computational efficiency. The overall numerical methods were validated by considering a fluid lens spreading between two other fluids.[22] Contact angles at the three-phase contact line were in good agreement with Young's relationship.[23] More details of the three-phase model will be published in the near future.

**Procedures**

To obtain reproducible and stable droplets, relevant printing parameters should be selected to operate under the optimum conditions. In this work, all aqueous droplet-generation experiments were carried out at velocities higher than 1–3 m/s at voltages of around 30–50 V (Fig. S3, ESI†), resulting in 60–100 pL droplets.

In the sequential-inkjet printing model, an oil drop array was first printed, followed by multiple precise injections of droplets with different compositions and volumes into those oil droplets in the required sequence. All the procedures were automatically controlled with a computer program. Oil droplet arrays can be fabricated in advance for future use: they can be preserved for long periods and even be tilted, flipped, or made to undergo a certain level of vibration without affecting the oil droplet form. In this work, all droplet-in-oil arrays were printed in a 10 × 10 spot format with spot-to-spot spacings of 400 μm. Because of the limited field of the fluorescence microscope with a 5× objective lens, only part of the droplet array could be detected at a time.

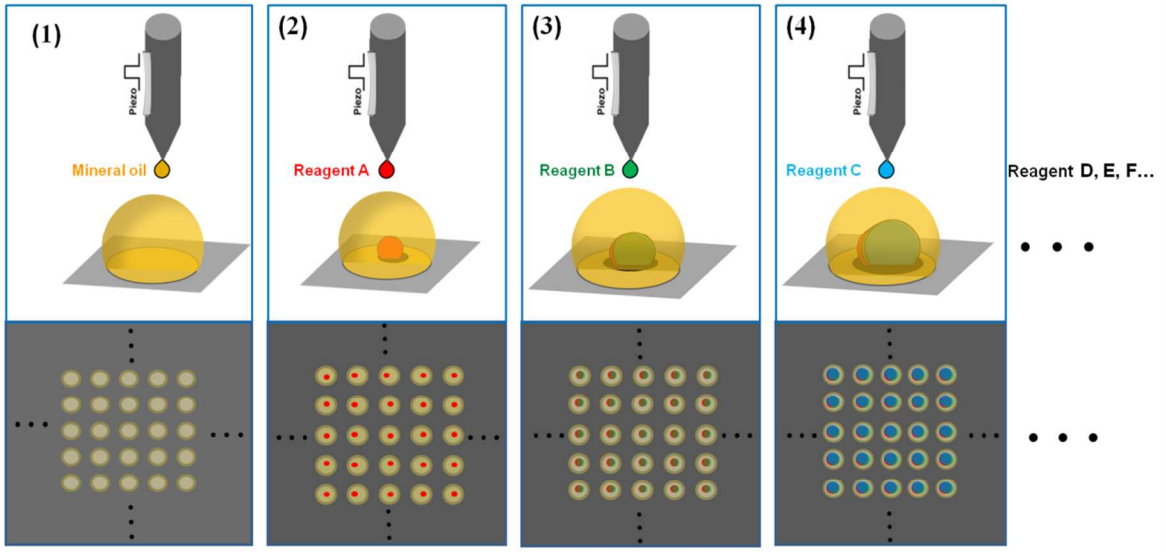


Figure 1. Schematic representation of picoliter droplet-in-oil array fabrication by sequential-inkjet printing on a silicon dioxide solid support. (1) Oil droplet array formation. (2) Reagent A is first dispensed on the oil microarray to produce the droplet-in-oil array. (3) Reagent B is then dispensed on the droplet-in-oil array, forming one larger droplet in the oil. (4) Reagent C is sequentially dispensed on the droplet-in-oil array, forming one larger droplet in the oil.

**Enzyme inhibition assay.** An enzyme inhibition assay was performed based on the sequential-inkjet printing model (Fig. 1). In this assay, the enzyme reaction medium was 10 mM Tris buffer with a pH of

7.3, adjusted using 0.1 M HCl. β-Galactosidase (β-gal, *E. coli*) was prepared in 10 mM Tris buffer with 0.1 mM $MgCl_2$ at pH 7.3 and stored frozen. The fluorogenic substrate FDG was stored frozen as a 10 mM stock solution in DMSO. The inhibitor DTPA was prepared and diluted with the same Tris buffer.[24]

## Results and Discussion

### Principles of Sequential-inkjet Printing

Sequential-inkjet printing adapts the inkjet printing platform to achieve efficient preparation of multicomponent droplet arrays on planar substrates for picoliter-scale analysis, under the premise of addressing the evaporation issues of picoliter droplets during the printing process without the assistance of solvents. The principles of the sequential-inkjet printing technique are presented schematically in Figure 1. (1) Mineral oil is first printed in a pattern on a silanized silicon dioxide surface with excellent hydrophobic and oleophobic properties using a 50 μm nozzle (Fig. 1-1). (2) A first-round printing of aqueous reagent A is performed on top of the preformed oil drops in the same pattern but with a 30 μm nozzle. The ejected droplets carrying reagent A penetrate the oil droplets at high velocity, overcoming their surface tension and viscosity. Subsequently, the aqueous droplets sink to the bottom of the less-dense mineral oil droplets, forming stable droplet-in-oil structures (Fig. 1-2). (3) During the second-pass printing of aqueous reagents, reagent B is inkjet-printed on the just-formed droplet-in-oil array of reagent A. Thus, the dispensed reagent B droplet also penetrates the oil drop due to its high velocity and immediately merges with the preformed droplet A inside the same oil drop (Fig. 1-3). (4) Additional reagents (C, D, E, etc.) can be respectively injected into the same oil drop by the foregoing method, as long as the oil drop is large enough not to burst (Fig. 1-4). By this approach, multicomponent droplet-in-oil structures can be assembled in a "penetration–merging–mixing" mode. When the droplet generation process is completed, the array is incubated for the reaction prior to detection with the fluorescence system.

### Model to Account for Sequential-inkjet Printing

Axisymmetric simulations were performed to study the droplet dynamics of the sequential-inkjet printing model, especially the effects of injection velocity on the success of droplet penetration. Some cases are noted herein.

**Velocity of droplet injection.** Figure 2a shows the dynamic droplet interaction processes for the case of droplet bouncing. The water droplet, with a velocity of 1 m/s, impacts the oil droplet at $t = t_3$, where its kinetic energy is transferred into the surface energy of the interface. Since the kinetic energy is insufficient to rupture the gas film, a thin gas film remains, separating the two droplets. This means that the oil/water interface cannot form. At $t = t_4$, the recovery motion of the oil droplet pushes the water droplet away, so that it bounces off the oil droplet at $t = t_6$. Subsequently, the water droplet falls onto the oil droplet under the effect of gravity, but again with insufficient velocity to rupture the gas film. Then, the water droplet floats on the top of the oil droplet in an unstable state. This model prediction shows good agreement with the video of a prior experiment, which shows the slipping of the water droplet on the surface of the oil droplet.[10]

Figure 2b shows the case in which the water droplet can penetrate the oil droplet. The water droplet impacts the oil surface at 2 m/s, and the gas film between the droplets is ruptured at $t = t_3$. Due to the large viscosity ratio between the oil and water droplets, most of the kinetic energy of the water droplet is dissipated in the oil phase during the impact. The subsequent engulfing is then controlled by imbalanced surface tension forces (the three surface tension values determine the position of the droplet at the interface).[25] In our case, the water/air surface tension is larger than the sum of the two other surface tensions. The water droplet will be engulfed by the oil droplet since the force balance at the triple point cannot be met.

The numerical simulations of unsuccessful and successful penetrations highlight the importance of surface tension relationships. If the engulfment condition induced by surface tension is met, the water droplet can penetrate the oil drop as long as they remain in contact. If the engulfment condition cannot be met, our additional simulations show that penetration will not occur, even at 10 m/s.

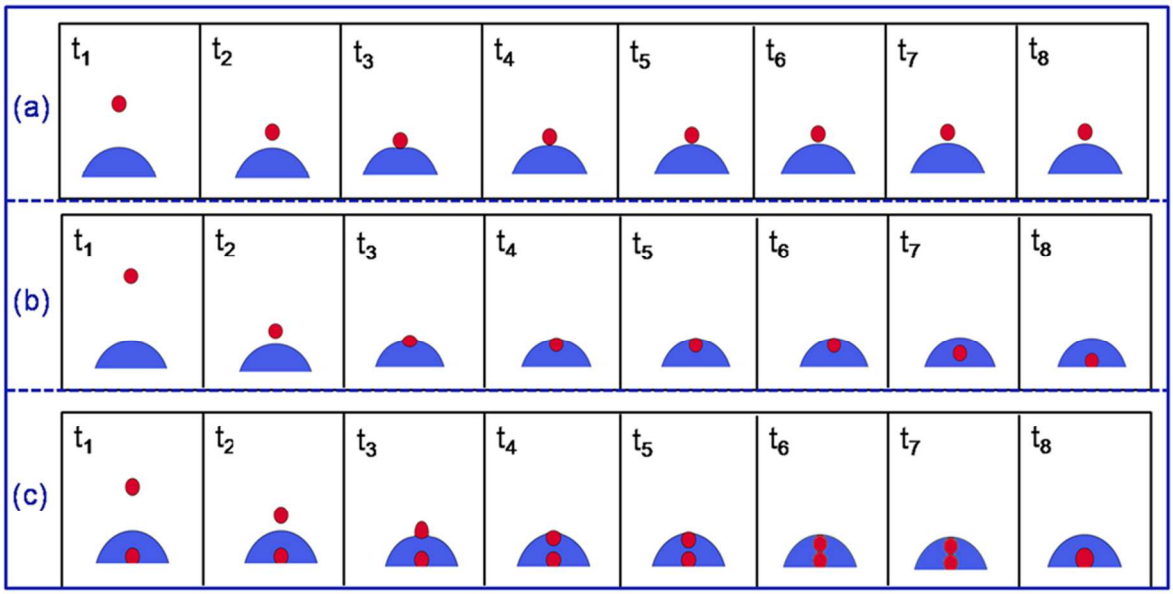


Figure 2. Simulation results for two cases of droplet-in-oil fabrication on a planar substrate. The oil and aqueous droplets are indicated by the blue and red shaded areas, respectively. (a) Dynamics of water droplet bouncing back from the oil droplet at a velocity of 1 m/s. (b) Dynamics of water droplet penetrating the oil droplet at a velocity of 2 m/s. (c) Dynamics of penetration of a second-round water droplet.

**Number of injection rounds.** We also found that after the first round of penetration by one liquid droplet, the required velocity was lower for a second-round droplet. Figure 2c shows the penetration of a second-round droplet at a velocity of 1 m/s. This result is due to the presence of the first droplet, which reduces the thickness of the oil phase. The deformation induced by the impact of the liquid droplet is thus larger. Consequently, the rupture of the gas film occurs earlier, which reduces the required impact velocity. Based on the model, a series of numerical simulation calculations were carried out for determining the critical velocity of water droplet injection in different rounds of droplet printing. As shown in Fig. 3a, the critical velocity decreases along with the increase in the number of inkjet printing rounds.

**Coalescence of droplets.** Figure 3b shows the mixing processes of water droplets in an oil drop. The diffusion of the reagents was restricted to isolate the effects of droplet impact. After penetrating the oil, droplets of reagent A lie on the bottom wall. A droplet of reagent B penetrates the oil droplet at $t = t_{a3}$ and merges with the droplet of reagent A at $t = t_{a4}$. Similar processes would occur with the further addition of aqueous reagents. After each injection, the mass of reagent B descends further toward the bottom wall through the center of reagent A. The contact area of the two reagents thus increases, enhancing their interaction. This type of flow evolution provides a valuable mixing effect between the droplets. Note that due to the high velocity of the injected droplet, the intense collision between the droplets may play an important role in stirring the preformed droplets, thus ensuring sufficient mixing. Theoretically, diffusion and the reaction process are also likely to enhance the mixing of the two reagents. The dual-fluorescence assay experiments also verified these simulation results, as discussed in the following section.

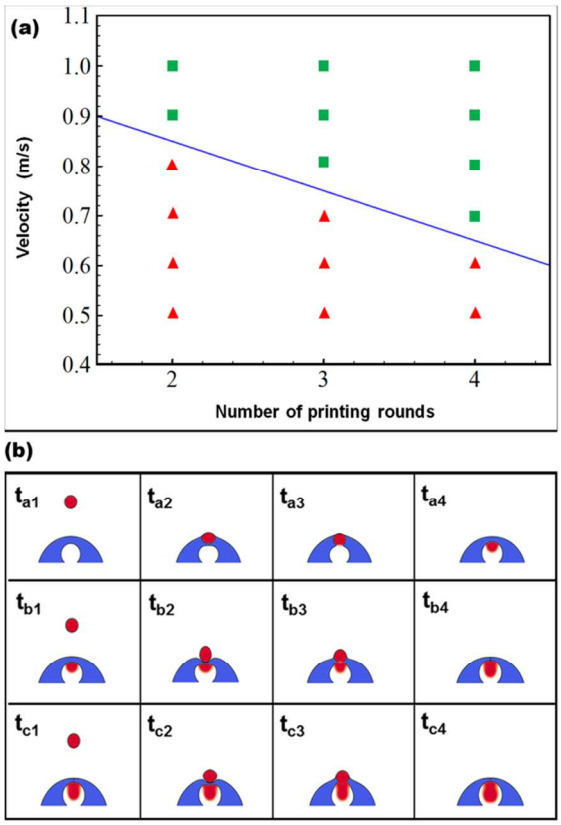


Figure 3. (a) Effect of existing water droplets on the velocity required for subsequent droplets. Green squares denote successful penetration; red triangles denote unsuccessful penetration. (b) Mixing processes of sequentially injected droplets. The oil drop and droplets of reagents A and B are indicated by the blue-, white-, and red-shaded areas, respectively.

**Feasibility of Sequential-inkjet Printing**

To demonstrate the feasibility and reliability of the sequential-inkjet printing model for multistep picoliter-scale droplet printing, we employed red ROX dye and green Alexa Fluor® 488 fluorescent dye as reagents (A) and (B), respectively. According to the schematic shown in Fig. 1, the ROX dye solution (300 pL) was first printed into the oil drop array (Fig. 4a), forming the droplet-in-oil array (Fig. 4b). Subsequently, the Alexa Fluor 488 solution (300 pL) was printed into the same oil array, forming a larger droplet-in-oil array (Fig. 4c). The entire two-step sequential-inkjet printing procedure is shown in Movie S1 (ESI†). The fluorescence images of the droplet-in-oil array during the sequential-inkjet printing procedure can be used to assess the consistency of the reagent droplets, both in spot morphology and fluorescence intensity. Figure 4b-3 shows the fluorescence of the first-round inkjet-printed array with the aqueous ROX dye, which exhibits only red fluorescence. Figures 4c-3 and 4c-4 show the second-round inkjet printing of aqueous Alexa Fluor® 488 dye in the same array, which now exhibits both red and green fluorescence. These results demonstrate the successful consecutive injection rounds and effective coalescence of the sequentially injected droplets containing different dyes.

We also investigated the fluorescence intensities of the reagent droplets during the sequential-inkjet printing procedures, and several significant conclusions were drawn based on the experimental data.

(1) As shown in Fig. 4c-2, only one aqueous droplet was contained in each oil drop, instead of two, indicating the successful fusion of the two injected droplets over two successive rounds of aqueous reagent printing. To evaluate the success rate of the droplets merging within one oil drop, a statistical trial was conducted on 200 droplet-in-oil samples generated by sequential-inkjet printing. It was found that the proportion of a single larger aqueous droplet in one oil drop reached as high as 98.4%, which indicates that the second-round droplet can not only efficiently penetrate the oil drop but also merge with the preformed first-round droplet with a reasonably high success rate. It is easy to understand these results: unlike droplet-based microfluidic systems in which surfactants are usually added in the oil phase to stabilize droplets against fusion,[26] no surfactant is used here. Thus, having once penetrated the oil, the ejected droplet can easily merge with the preformed droplet upon contact, as a result of surface tension.

(2) As shown in Fig. 4d, due to the secondary injection of Alexa Fluor 488 solution in the same volume, the red fluorescence intensity of the droplet decreased by about half, which also confirms the reliability of the sequential-inkjet printing method. Furthermore, both the red and green fluorescence intensities were uniformly distributed in the aqueous droplet, which revealed that the two droplets achieved sufficient mixing. These results indirectly validated our simulation results.

(3) The fluorescence intensity of the droplet will be significantly different for the successful and failed droplets-in-oil based on sequential-inkjet printing. The relative standard deviation (RSD) of the fluorescence intensity was measured to

demonstrate the uniformity of the aqueous droplet sizes in the oil drops. In a statistical analysis of 200 droplet-in-oil samples, the homogeneity of the green fluorescence array was greater than that of the red, which is consistent with the RSD values of the droplet arrays, 4.1% and 7.8%, respectively. This indirectly indicates that the second-round injection more easily penetrates the oil drop than the first, which is coincident with the simulation results described in the previous section. Consequently, we conclude that the success rate of multiple injections would increase with an increase in the number of inkjet printing rounds. This characteristic could be of important value for multistep analyses with continuous reagent addition.

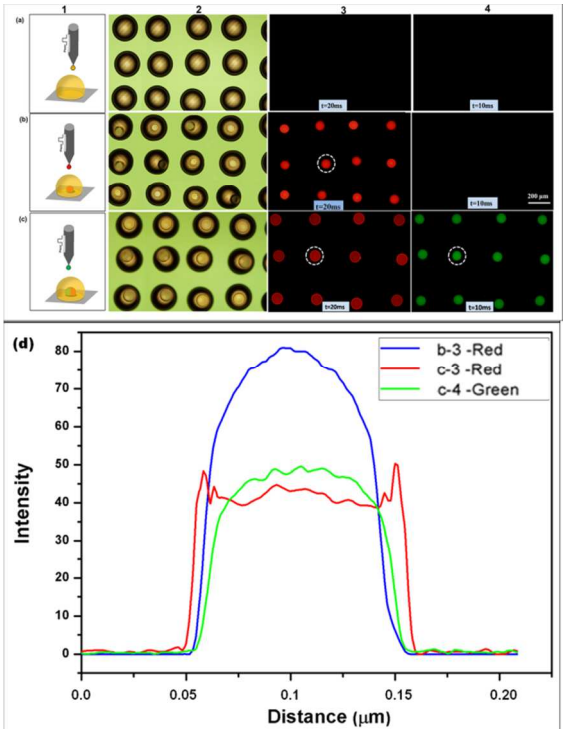


Figure 4. Procedure for the two-step sequential-inkjet printing used to construct the dual-fluorescence assay system. Row (a) shows the mineral oil array. Row (b) shows the first-round droplet-in-oil array after 300 pL ROX dye was inkjet-printed into the oil droplets. Row (c) shows the same second-round droplet-in-oil array after 300 pL Alexa Fluor 488 solution was inkjet-printed into the droplet-in-oil array in row (b) containing the ROX droplet. The four columns (1–4) from left to right display schematic diagrams, bright-field images, and the corresponding fluorescence images, respectively. (d) Relative fluorescence intensities of the three droplets indicated by white circles in Fig. 4b and Fig. 4c. The blue line represents the red fluorescence intensity of one aqueous droplet containing ROX dye solution (Fig. 4b-3). The red and green lines represent the red and green fluorescence intensities of the same aqueous droplet containing ROX and Alexa Fluor 488 solutions (Figs. 4c-3 and 4c-4).

**Enzyme Inhibition Assays**

We also applied the sequential-inkjet printing model in an enzyme inhibition assay. This assay was based on the inhibition of β-galactosidase by inhibitor (DTPA) solutions with different concentrations, impeding the enzyme-mediated conversion of substrate FDG into fluorescent hydrolysates (FMG) and fluorescein.[27] A series of droplet-in-oil microreactors with the same enzyme and substrate concentrations and different inhibitor concentrations was assembled according to Fig. 1 in the following steps (Fig. 5a–d): (1) mineral oil drops array (3 nL); (2) DTPA droplets (200 pL, 100 μM); (3) β-gal droplets (200 pL, 0.1 mg/mL); and (4) FDG droplets (200 pL). During the droplet-array generation process, the microchip was kept at a relatively low temperature (4°C) to minimize the enzyme reaction before incubation. Accordingly, we obtained a final array of 600 pL droplets-in-oil, which presented different fluorescence intensities (Fig. 5d-3). To ensure the reliability of the enzyme inhibition results, each compound was tested in decuplicate, and the average results for the 30 droplet reactors after incubation were determined. Previously,[10] we verified that the final droplet-in-oil structure was stable for more than 2 h without changing the shape and volume, which was sufficient to allow for the multiple dispensing (20 min) and incubating processes (20 min).

Figure 5e and 5f displays the results of enzyme inhibition assays in the range of 0–5.0 mM DTPA. The average values of the fluorescence intensities of the droplets were measured with ImageJ (Fig. 5d-3). The percentage of inhibition (PI)[28] in the range of 0–5.0 mM DTPA was calculated on the basis of the fluorescence intensity, assuming the intensity of 0 mM DTPA to be 100% (*i.e.*, 0% inhibition). The inhibition curve is shown in Figure 5f. The $IC_{50}$ value (the half maximal inhibitory concentration) deduced from this curve is 0.76 mM DTPA. These results are comparable with those previously reported,[1] consequently proving the reliability and effectiveness of this novel sequential-inkjet printing method for the screening of multiple samples in picoliter-scale droplet-in-oil structures. What's more, compared with previous inkjet printing process[29,30,31] which can compromise enzymatic activity during compression stresses and shear stresses in the stage of droplet formation, the droplet velocities here employed are sufficiently low (1-3 m/s) that these stresses can be neglected in principle, which

Lab on a Chip

ARTICLE

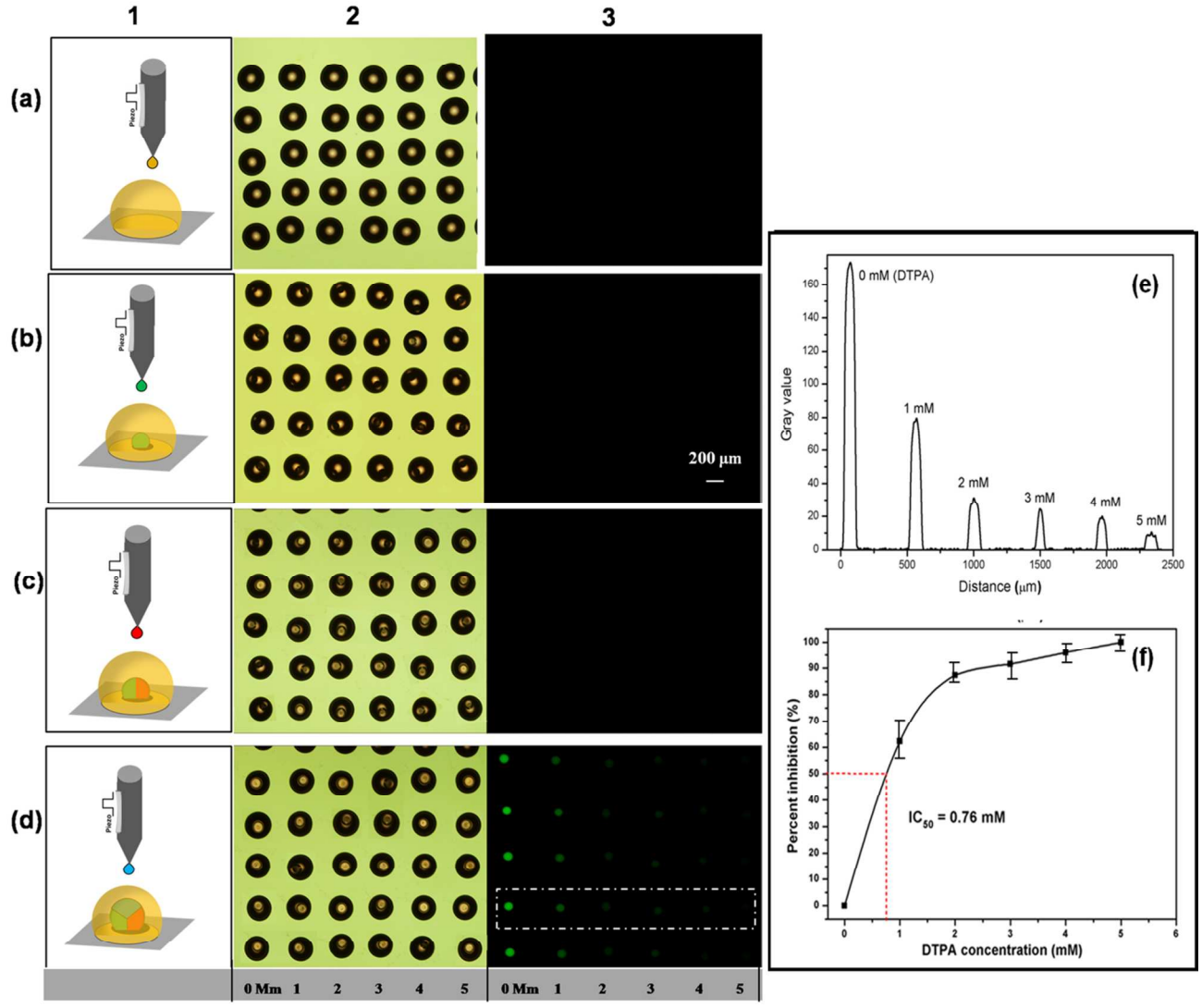


Figure 5. Three-step sequential-inkjet printing procedure for the enzyme inhibition assay. Bright-field images (column 2) and fluorescence images (column 3) show the complete formation process of a picoliter droplet-in-oil array for enzyme inhibition. In row (a), a 5 × 6 array was generated with 3 nL mineral oil droplets. Row (b) shows the first-round droplet-in-oil array after 200 pL β-galactosidase was inkjet-printed into the oil droplets. Row (c) shows the same second-round droplet-in-oil array after 200 pL DTPA inhibitor solutions at concentrations of 0–5.0 mM were inkjet-printed into the droplet-in-oil array in row (b) containing the enzyme. Row (d) shows the same third-round droplet-in-oil array after 200 pL FDG used as the substrate was inkjet-printed into the droplet-in-oil array in row (c) containing the enzyme and inhibitor. (e) Relative fluorescence intensities in the row of droplets shown in Fig. 5d-3. (f) Inhibition curve obtained from Fig. 5e. Scale bars: 200 µm.

coincides well with the experimental results.

## Conclusions

We have developed a model to describe the multiple injection procedure of sequential-inkjet printing, as well as validated the design in a two-step fluorescence assay and a three-step enzyme inhibition assay. The proposed method exhibits good performance with respect to multiple injections, successful droplet coalescence, and rapid mixing, which is significant for multistep screening. Compared with the reported inkjet printing systems[11,12] for

automated screening with nanoliter or picoliter precision, the sequential-inkjet printing model provides reliable multistep droplet printing while exhibiting all of the following features: non-contact liquid dispensing capability, absence of evaporation issues without the aid of additives, and capability for multistep/sequential droplet assembly. While double-inkjet printing has been demonstrated previously to avoid evaporation during picoliter droplet printing,[9] this work extends the previous approach with new research, including (i) the development of a model for studying droplet dynamics in sequential-inkjet printing, leading to several important conclusions; and (ii) the first demonstration using inkjet printing technology to implement multistep droplet injections based on the droplet-in-oil structure. We believe that applying this sequential-inkjet printing methodology to existing inkjet printing devices will enhance their use as universal diagnostic tools as well as accelerate the adoption of inkjet printing in multistep screening experiments. However, this method is still obviously inadequate, requiring further study and improvement in future work. As follow-ups to this study, we will focus on two aspects: (i) optimizing the formulation for high-throughput droplet-in-oil printing. We are now working on identifying the appropriate proportion of emulsifiers in the oil phase to improve the success of droplet-in-oil printing. (ii) Directly validating our simulation model by obtaining high-speed videos of the sequential inkjet-printing process. We believe that once we solve the large-scale droplet-in-oil array fabrication problem, this sequential-inkjet printing method will be widely applied not only for the high-throughput screening of compound libraries, but also in other important areas such as protein crystallization, immunoassays, and single-cell assays.

## Acknowledgements

This work was supported by grants from the Instrument Development Project of the Chinese Academy of Sciences (Grant No. 61334008), the National Natural Science Foundation of China (Grant No. 11402274), and the Scientific and Technological Innovation “Interdiscipline and Cooperation Team” Project of the Chinese Academy of Sciences, 2012. Prof. Jinling Yang and Mr. Yutao Zheng are gratefully acknowledged for their support in the design and operation of the inkjet printing system for droplet-in-oil fabrication.

## Notes and references

1 G. Arrabito, C. Musumeci, V. Aiello, S. Libertino, G. Compagnini and B. Pignataro, *Langmuir,* 2009, **25**, 6312.
2 G. Arrabito and B. Pignataro, *Anal. Chem.,* 2010, **82**, 3104.
3 G. Arrabito, C. Galati, S. Castellano and B. Pignataro, *Lab Chip,* 2013, **13**, 68.
4 F. Chen, S. Mao, H. Zeng, S. Xue, J. Yang, H. Nakajima, J.M. Lin and K. Uchiyama, *Anal. Chem*., 2013, **85**, 7413.
5 H. Kim, S. Vishniakou and G. W. Faris, *Lab Chip,* 2009, **9**, 1230.
6 Y. Zhang, Y. Zhu, B. Yao and Q. Fang, *Lab Chip,* 2011, **11**, 1545.
7 D. N. Gosalia and S. L. Diamond, *Proc. Natl. Acad. Sci.,* 2003, **100**, 8721.
8 L. Mugherli, O. N. Burchack, L. A. Balakireva, A. Thomas, F. Chatelain and M. Y. Balakirev, *Angew. Chem.,* 2009, **121**, 7775.
9 T. Arakawa, Y. S. Kitaand and N. Timasheff, *Biophys. Chem.,* 2007, **131**, 62.
10 Y. N. Sun, X. G Zhou and Y. D. Yu, *Lab Chip,* 2014, **14**, 3603.
11 W. B. Du, M. Sun, S. Q. Gu, Y. Zhu and Q. Fang, *Anal. Chem.,* 2010, **82**, 9941.
12 T. R. Thorsen, W. Roberts, F. H. Arnold and S. R. Quake, *Phys. Rev. Lett.* 2001, **86**, 4163.
13 T. Nisisako, T. Torii and T. Higuchi, *Lab Chip.* 2002, **2**, 24.
14 D. R. Link, S. L. Anna, D. A. Weitz and H. A. Stone, *Phys. Rev. Lett.* 2004, **92**, 054503.
15 S. L. Anna, N. Bontoux and H. A. Stone, *Appl. Phys. Lett.* 2003, **82**, 364.
16 Y. Zhu, Y. X. Zhang, L. F. Cai and Q. Fang, *Anal. Chem*., 2013, **85**, 6723.
17 Y. Zhu, L. N. Zhu, R. Guo, H. J. Cui, S. Ye and Q. Fang, *Sci. Rep.,* 2014, **4**, 5046.
18 C. J. Beverung, C. J. Radke and H. W. Blanch, *Biophys. Chem.,* 1999, **81**, 59.
19 MicroFab Technologies, http://www.microfab.com/ ( accessed May 2014).
20 S. J. Popinet, *Comp. Phys.,* 2009, **228**, 5838.
21 X. Chen and V. J. Yang, *Comp. Phys.,* 2014, **269***,* 22.
22 F. Boyer, C. Lapuerta, S. Minjeaud, B. Piar and M. Quintard, *Trans. Porous Media,* 2010, **82**, 463.
23 T. Young, Philos. Trans. R. Soc. London, 2004, **95**, 65.
24 W. B. Du, Q. Fang and Z. L. Fang, *Anal. Chem*., 2006, **78**, 6404.
25 J. Berthier and K. A. Brakke, in *The Physics of Microdroplets,* Wiley, 2012.
26 J. C. Baret, *Lab Chip,* 2012, **12**, 422.
27 Q. S. Pu and S. R. Liu, *Anal. Chim. Acta,* 2004, **511**, 105.
28 A. G. Hadd, D. E. Raymond, J. W. Halliwell, S. C. Jacobson and J. M. Ramsey, *Anal. Chem.,* 1997, **69,** 3407.
29 G. M. Nishioka, A. A. Markey and C. K. Holloway, *JACS*, 2004, **126**, 16320.
30 G. Arrabito, C. Musumeci, V. Aiello, S. Libertino, G. Compagnini and B. Pignataro, *Langmuir*, 2009, **25**, 6312.
31 H. Dong, W. W. Carr and J. F. Morris, *Phys of Fluids*, 2006, **18**, 072102.



 